

A targeted theranostic platinum(IV) prodrug containing a luminogen with aggregation-induced emission (AIE) characteristics for *in situ* monitoring of drug activation†

 Cite this: *Chem. Commun.*, 2014, 50, 3868

 Received 16th December 2013,
 Accepted 19th February 2014

DOI: 10.1039/c3cc49516g

 Youyong Yuan,‡^a Yilong Chen,‡^b Ben Zhong Tang*^{b,c} and Bin Liu*^{a,d}

www.rsc.org/chemcomm

A targeted theranostic platinum(IV) prodrug based on a luminogen with aggregation-induced emission (AIE) characteristics was developed for selective and real-time monitoring of drug activation *in situ*.

Cisplatin has been widely used in clinics to treat a broad range of human malignancies. However, like most other cytotoxic anti-cancer drugs, its clinical use is often limited due to severe side effects.¹ To address these limitations, researchers have developed a promising alternative strategy by using non-toxic Pt(IV) prodrugs, which can be intracellularly activated by reduction to Pt(II) complex and restore their latent cytotoxic activity.² Although the use of Pt(IV) prodrug has been proved to be successful in improving the efficacy of platinum-based drugs, it remains a challenge to elucidate how and when Pt(IV) prodrugs are reduced after cell internalization.

To date, fluorescent techniques remain the most effective strategy for monitoring the intracellular reduction process of platinum(IV) complex.³ The most direct method in studying platinum reduction is by attaching fluorophore–quencher pairs to the two ligands of Pt(IV) complexes, which can restore the fluorescence due to prodrug reduction induced donor–acceptor separation.^{3a–c} However, very few systems have been successfully utilized in living cell imaging.^{3d,e} It is highly desirable that one be able to design and develop a theranostic system which can specifically deliver the Pt(IV) prodrugs and simultaneously perform real-time monitoring of the drug activation *in situ*, which can provide a quantitative readout of dynamic processes in living cells.

Luminogens with aggregation-induced emission (AIE) characteristics have offered a powerful and versatile tool for biosensing

and bioimaging.⁴ They are non-emissive in the molecularly dissolved state, but induced to emit bright fluorescence by aggregation due to the restriction of intramolecular rotations (RIR) and prohibition of energy dissipation *via* non-radiative channels.⁵ Recently, we have developed AIE luminogen based light-up probes for monitoring of cellular molecules.⁶ However, reports describing theranostic drug conjugate based on these molecules have not yet been published.

In this communication, we report the synthesis and biological evaluation of a targeted theranostic platinum(IV) prodrug delivery system based on an AIE luminogen for *in situ* monitoring of the platinum(IV) prodrug activation. The theranostic system is composed of a chemotherapeutic prodrug Pt(IV), which can be reduced to active Pt(II) inside the cells, a tetraphenylethene pyridinium (PyTPE) unit with AIE characteristics, a short hydrophilic peptide with five aspartic acid (D5) units to ensure its water solubility^{6b} and a cyclic arginine–glycine–aspartic acid (cRGD) tripeptide as a targeting ligand (Scheme 1). The prodrug is highly water-soluble and can accumulate preferentially in cancer cells that overexpress $\alpha_v\beta_3$ integrin. In aqueous media, the AIE moiety is non-fluorescent due to the high hydrophilicity of the D5-cRGD, but its emission is enhanced significantly after the reduction of the Pt(IV) complex to active Pt(II) drug. The fluorescence enhancement (“turn-on”) is attributed to the restriction of intramolecular rotations of the PyTPE phenyl rings in the cleaved residues, which populates the radiative decay channels. Our prodrug design offers good opportunity for efficient platinum

^a Department of Chemical and Biomolecular Engineering, National University of Singapore, 4 Engineering Drive 4, Singapore 117576. E-mail: cheliub@nus.edu.sg

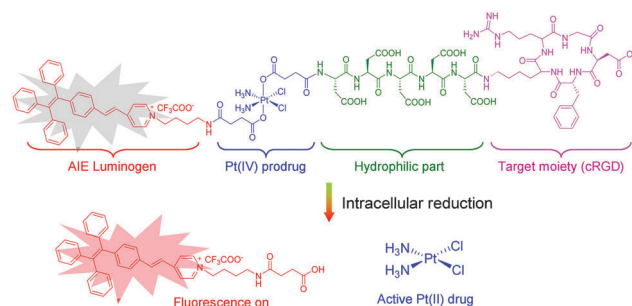
^b Department of Chemistry, Division of Biomedical Engineering, The Hong Kong University of Science and Technology, Clear Water Bay, Kowloon, Hong Kong. E-mail: tangbenz@ust.hk

^c SCUT-HKUST Joint Research Laboratory, Guangdong Innovative Research Team, State Key Laboratory of Luminescent Materials and Devices, South China University of Technology, Guangzhou, 510640, China

^d Institute of Materials Research and Engineering, 3 Research Link, Singapore 117602

† Electronic supplementary information (ESI) available: Detailed experimental methods and additional data. See DOI: 10.1039/c3cc49516g

‡ These authors contribute equally.



Scheme 1 Schematic illustration of prodrug PyTPE–Pt–D5–cRGD design strategy and the fluorescence turn-on monitoring of drug activation.

drug delivery and real-time monitoring of the drug activation with a high signal-to-noise ratio.

Amine-functionalized PyTPE (PyTPE-NH₂) was synthesized by reducing azide-PyTPE (PyTPE-N₃) in methanol (Scheme S1 and Fig. S1 and S2, ESI[†]). Pentafluorophenol-activated Pt(IV) complex was prepared from commercially available anticancer drug cisplatin and was used as the linker (Scheme S2 and Fig. S3–S5, ESI[†]). The synthetic route for the prodrug PyTPE-Pt-D5-cRGD is shown in Scheme S3 (ESI[†]). Asymmetric functionalization of activated Pt(IV) complex with PyTPE-NH₂ and amine-functionalized peptide D5-cRGD in the presence of *N,N*-diisopropylethylamine afforded the prodrug in 42% yield. A control prodrug PyTPE-Pt-D5 with a similar structure but without cRGD moiety was also synthesized in 44% yield (Scheme S4, ESI[†]). In addition, a non-activatable control PyTPE-C6-D5-cRGD was prepared in 46% yield by using disuccinimidyl suberate to replace activated Pt(IV) complex in the coupling reaction (Scheme S5, ESI[†]). The NMR and MS characterization confirmed the right structures of the compounds with high purity (Fig. S6–S14, ESI[†]).

To evaluate PyTPE-Pt-D5-cRGD as a potential anticancer drug, we first studied the nature of the formed Pt(II) species upon reduction. Previous studies have shown that diethyldithiocarbamate (DDTC) can react with Pt(II) complexes to yield the adduct of Pt(DDTC)₂ but not with the stable Pt(IV) complexes.⁷ LC-mass was subsequently used to monitor the adduct formation between Pt(II) and DDTC. Ascorbic acid was selected because it has been reported to be one of the major reducing agents for the reduction of Pt(IV) in cells.^{2b} As shown in Fig. 1A, free DDTC has a retention time of 13.3 min, which is slightly shorter than that of Pt(DDTC)₂ (14.4 min). In the absence of ascorbic acid, there is no peak formed for Pt(DDTC)₂ when PyTPE-Pt-D5-cRGD is incubated with DDTC. Only in the presence of ascorbic acid, the prodrug can react with DDTC to form Pt(DDTC)₂ with a mass-to-charge ratio (*m/z*) of 492.104 (Fig. S15, ESI[†]), confirming that the released Pt entities are indeed Pt(II) species. Another piece of evidence is that a peak at 14.1 min with a *m/z* of 1140.344 (Fig. S16, ESI[†]) is found for PyTPE-COOH (Scheme S6, ESI[†]) after reduction. These results indicate that the prodrug can be reduced by ascorbic acid to generate the active Pt(II) drug and release the axial moieties simultaneously.

The UV-vis absorption spectra of PyTPE-NH₂ in THF and PyTPE-Pt-D5-cRGD in DMSO/PBS (phosphate buffered saline) mixtures (*v/v* = 1/199) are shown in Fig. S17 (ESI[†]). Both have a similar absorption profile in the range of 348–500 nm with a maximum at 405 nm. The photoluminescence (PL) spectra of PyTPE-NH₂ and PyTPE-Pt-D5-cRGD in DMSO/PBS (*v/v* = 1/199) are shown in Fig. 1B. The hydrophobic PyTPE-NH₂ shows intense fluorescence while PyTPE-Pt-D5-cRGD is almost non-fluorescent in the same mixture, due to easy intramolecular rotations of the TPE phenyl rings in aqueous media. The significant difference in the PL intensities of PyTPE-NH₂ and PyTPE-Pt-D5-cRGD offers opportunity for the prodrug to be used for real-time monitoring of the drug activation.

To study the response of the prodrug upon reduction, we incubated PyTPE-Pt-D5-cRGD (10 μM) with ascorbic acid (1 mM) in DMSO/PBS (*v/v* = 1/199), and the fluorescence spectra were measured at different time points. As shown in Fig. 1C, the emission intensity of PyTPE-Pt-D5-cRGD increases significantly with time, reaching the plateau in 1.5 h, which is 18-fold higher than the emission from

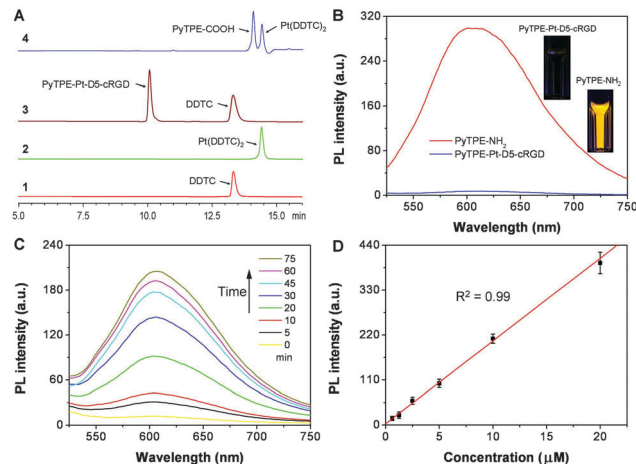


Fig. 1 (A) HPLC chromatograms showing the reaction of DDTC with cisplatin and reduced Pt(IV) prodrug: (1) DDTC alone; (2) the reaction between DDTC and cisplatin; (3) the reaction between DDTC and PyTPE-Pt-D5-cRGD; (4) the reaction between DDTC and PyTPE-Pt-D5-cRGD (10 μM) in the presence of ascorbic acid (1 mM) for 12 h. (B) PL spectra of PyTPE-NH₂ and PyTPE-Pt-D5-cRGD in DMSO/PBS mixtures (*v/v* = 1/199). Inset: the corresponding photographs taken under illumination of a UV lamp at 365 nm. (C) Time-dependent PL spectra of PyTPE-Pt-D5-cRGD (10 μM) treated with ascorbic acid (1 mM). (D) Plot of PL intensity at 605 nm versus concentrations of PyTPE-Pt-D5-cRGD with the incubation of ascorbic acid (1 mM) for 75 min in DMSO/PBS (*v/v* = 1/199). Data represent mean values ± standard deviation, *n* = 3.

the prodrug itself. The non-targetable prodrug PyTPE-Pt-D5 shows a similar fluorescence intensity increase after incubation under the same conditions (Fig. S18A, ESI[†]). In contrast, negligible fluorescence intensity increase is observed for PyTPE-C6-D5-cRGD (Fig. S18B, ESI[†]). Further titration of PyTPE-Pt-D5-cRGD with other bio-acids and proteins showed negligible fluorescence intensity change, indicating high stability of the prodrug (Fig. S19, ESI[†]). Only in the presence of the reducing agent (glutathione or ascorbic acid), the prodrug showed an intense fluorescence change. These results indicate that the fluorescence enhancement is attributed to the reduction of the prodrug with the release of AIE residue (PyTPE-COOH).

Next, we incubated different concentrations of PyTPE-Pt-D5-cRGD with ascorbic acid (1 mM) and the fluorescence intensities of the prodrug were monitored. The plot of the PL intensities at 605 nm against the prodrug concentration is perfectly linear (Fig. 1D and Fig. S20, ESI[†] for PyTPE-Pt-D5), suggesting the possibility of quantification of the activated Pt(II) drugs. The gradually enhanced fluorescence intensities are due to the increased amounts of PyTPE aggregates formed in aqueous media. The molecular dissolution of the probe and the aggregate formation of the cleaved products were confirmed by laser light scattering (LLS) measurements. In the aqueous mixture, no LLS signals could be detected from the solution of PyTPE-Pt-D5-cRGD. However, after the reduction, the residual hydrophobic AIE luminogen clusters into aggregates with an average diameter of 145 nm (Fig. S21, ESI[†]). Therefore, the drug activation process can be easily monitored on the basis of the PL intensity changes.

The cell lysates of breast cancer cells MDA-MB-231 were directly incubated with PyTPE-Pt-D5-cRGD (10 μM) and the fluorescence intensity at 605 nm was monitored over time. As shown in Fig. S22 (ESI[†]), the fluorescence intensity increases quickly in a similar way to

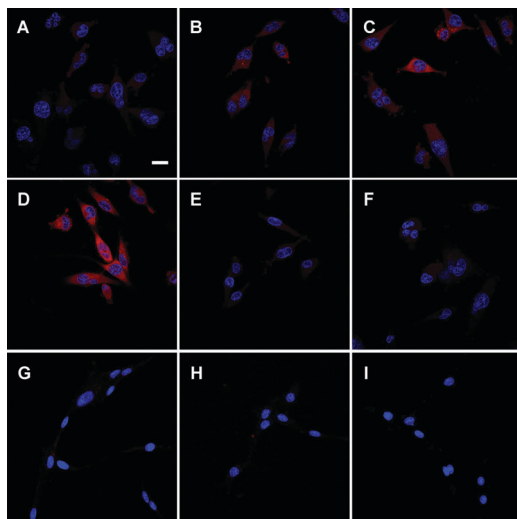


Fig. 2 Confocal images of MDA-MB-231 (A–F) and MCF-7 (G–I) cells after incubation with PyTPE-Pt-D5-cRGD for 1 h (A), 2 h (B), 4 h (C), 6 h (D, G); PyTPE-Pt-D5 for 6 h (E, H) and PyTPE-C6-D5-cRGD for 6 h (F, I). The nuclei were stained with Hoechst 33342. All images share the same scale bar (20 μm).

that of the solution study with ascorbic acid in Fig. 2C. Meanwhile, the fluorescence intensity shows a minimum change after incubation PyTPE-C6-D5-cRGD with the lysate, indicating that the prodrug is highly stable in the environment containing cellular proteins.

To explore the capability of using PyTPE-Pt-D5-cRGD to monitor intracellular drug reduction in cancer cells, the prodrug was incubated with MDA-MB-231 and MCF-7 breast cancer cells. The confocal imaging results are shown in Fig. 2. MDA-MB-231 cells with over-expressed integrin $\alpha_v\beta_3$ on the cellular membrane were chosen as integrin-positive cancer cells, while MCF-7 cells with a low level of integrin $\alpha_v\beta_3$ expression were used as the negative control. As shown in Fig. 2, after the incubation with PyTPE-Pt-D5-cRGD, the fluorescence in MDA-MB-231 cells is increased gradually with time and reaches a plateau in 6 h, whereas for MCF-7 cells only a weak fluorescent signal could be detected even after 6 h incubation. In contrast, PyTPE-Pt-D5 displays weak fluorescence for both cell lines (Fig. 2E and H), which might be due to the inefficient cellular uptake of both cells. These results further strengthen the targeting ability of PyTPE-Pt-D5-cRGD. When MDA-MB-231 cells were pre-treated with free cRGD prior to PyTPE-Pt-D5-cRGD incubation, the image shows weak fluorescence (Fig. S23, ESI[†]). The marked difference reveals that the selective uptake of PyTPE-Pt-D5-cRGD by MDA-MB-231 cells is due to the integrin receptor-mediated process. For PyTPE-C6-D5-cRGD, almost no detectable fluorescence was observed after 6 h incubation (Fig. 2F and I).

We next studied the cytotoxicity profile of the prodrug to MDA-MB-231 and MCF-7 cells by a MTT assay. As shown in Fig. 3A, PyTPE-Pt-D5-cRGD shows obvious cytotoxicity to MDA-MB-231 cells, while in a parallel experiment for MCF-7 cells, it shows minimum toxicity. The half-maximal inhibitory concentration (IC_{50}) of PyTPE-Pt-D5-cRGD towards MDA-MB-231 cells is 30.2 μM . In addition, PyTPE-Pt-D5 and PyTPE-C6-D5-cRGD do not show obvious cytotoxicity to both cells. As MDA-MB-231 and MCF-7 cells were reported to show a similar IC_{50} value toward cisplatin,⁸ these results indicate that the cRGD moiety is able to guide the prodrug to $\alpha_v\beta_3$ integrin overexpressed tumor cells, resulting in selective cell death.

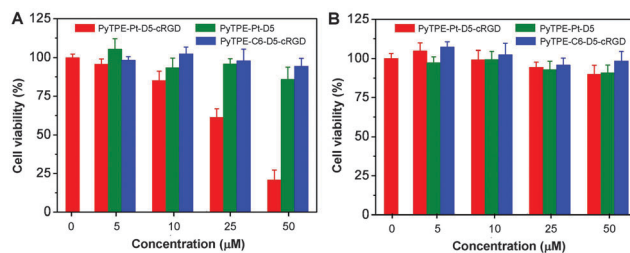


Fig. 3 Cell viability of MDA-MB-231 (A) and MCF-7 (B) cells upon treatment with PyTPE-Pt-D5-cRGD, PyTPE-Pt-D5 and PyTPE-C6-D5-cRGD at different concentrations for 72 h. Data represent mean values \pm standard deviation, $n = 3$.

In conclusion, we report the synthesis and biological applications of a fluorescent light-up prodrug based on an AIE luminogen for real-time monitoring of drug activation inside the cells. Thanks to the unique nature of the AIE luminogen, the prodrug is non-fluorescent in aqueous media but becomes highly emissive when reduced inside the cells. Similar to the cRGD functionalized prodrug which allows for selective targeting of $\alpha_v\beta_3$ integrin on many angiogenic cancers, replacing cRGD with other tumor receptor specific ligands will be likely to yield more functionalized prodrugs for selective killing of different cancer cells. The capability of monitoring prodrug activation processes through fluorescence changes of AIE fluorogen offers a new opportunity for the development of theranostic anti-cancer therapeutics.

We thank the Singapore National Research Foundation (R-279-000-390-281), the Ministry of Defense (R279-000-340-232), the Research Grants Council of Hong Kong (HKUST2/CRF/10 and N_HKUST620/11), and the JCO (IMRE/12-8P1103).

Notes and references

- V. Pinzani, F. Bressolle, I. J. Haug, M. Galtier, J. P. Blayac and P. Balmes, *Cancer Chemother. Pharmacol.*, 1994, **35**, 1–9.
- (a) X. Y. Wang and Z. J. Guo, *Chem. Soc. Rev.*, 2013, **42**, 202–224; (b) N. Graf and S. J. Lippard, *Adv. Drug Delivery Rev.*, 2012, **64**, 993–1004.
- (a) E. J. New, R. Duan, J. Z. Zhang and T. W. Hambley, *Dalton Trans.*, 2009, 3092–3101; (b) C. Molenaar, J. M. Teuben, R. J. Heetebrij, H. J. Tanke and J. Reedijk, *J. Biol. Inorg. Chem.*, 2000, **5**, 655–665; (c) J. J. Wilson and S. J. Lippard, *Inorg. Chim. Acta*, 2012, **389**, 77–84; (d) Y. Song, K. Suntharalingam, J. S. Yeung, M. Royzen and S. J. Lippard, *Bioconjugate Chem.*, 2013, **24**, 1733–1740; (e) D. Montagner, S. Q. Yap and W. H. Ang, *Angew. Chem., Int. Ed.*, 2013, **52**, 11785–11789.
- (a) D. Ding, K. Li, B. Liu and B. Z. Tang, *Acc. Chem. Res.*, 2013, **46**, 2441–2453; (b) C. W. Leung, Y. Hong, S. Chen, E. Zhao, J. W. Lam and B. Z. Tang, *J. Am. Chem. Soc.*, 2013, **135**, 62–65; (c) J. Geng, K. Li, W. Qin, L. Ma, G. G. Gurzadyan, B. Z. Tang and B. Liu, *Small*, 2013, **9**, 2012–2019; (d) X. H. Huang, X. G. Gu, G. X. Zhang and D. Q. Zhang, *Chem. Commun.*, 2012, **48**, 12195–12197; (e) Z. Wang, S. Chen, J. W. Y. Lam, W. Qin, R. T. K. Kwok, N. Xie, Q. Hu and B. Z. Tang, *J. Am. Chem. Soc.*, 2013, **135**, 8238–8245; (f) F. F. Wang, J. Y. Wen, L. Y. Huang, J. J. Huang and O. Y. Jin, *Chem. Commun.*, 2012, **48**, 7395–7397; (g) T. Y. Han, X. Feng, B. Tong, J. B. Shi, L. Chen, J. G. Zhi and Y. P. Dong, *Chem. Commun.*, 2012, **48**, 416–418.
- (a) Y. N. Hong, J. W. Y. Lam and B. Z. Tang, *Chem. Commun.*, 2009, 4332–4353; (b) Y. N. Hong, J. W. Y. Lam and B. Z. Tang, *Chem. Soc. Rev.*, 2011, **40**, 5361–5388.
- (a) H. B. Shi, R. T. K. Kwok, J. Z. Liu, B. G. Xing, B. Z. Tang and B. Liu, *J. Am. Chem. Soc.*, 2012, **134**, 17972–17981; (b) Y. Y. Yuan, R. T. K. Kwok, G. X. Feng, J. Liang, J. L. Geng, B. Z. Tang and B. Liu, *Chem. Commun.*, 2014, **50**, 295–297.
- J. Li, S. Q. Yap, C. F. Chin, Q. Tian, S. L. Yoong, G. Pastorin and W. H. Ang, *Chem. Sci.*, 2012, **3**, 2083–2087.
- S. M. Lee, T. V. O'Halloran and S. T. Nguyen, *J. Am. Chem. Soc.*, 2010, **132**, 17130–17138.